UNCLASSIFIED

AD 295 192

Reproduced
by the

ARMED SERVICES TECHNICAL INFORMATION AGENCY
ARLINGTON HALL STATION
ARLINGTON 12, VIRGINIA

UNCLASSIFIED

NOTICE: When government or other drawings, specifications or other data are used for any purpose other than in connection with a definitely related government procurement operation, the U. S. Government thereby incurs no responsibility, nor any obligation whatsoever; and the fact that the Government may have formulated, furnished, or in any way supplied the said drawings, specifications, or other data is not to be regarded by implication or otherwise as in any manner licensing the holder or any other person or corporation, or conveying any rights or permission to manufacture, use or sell any patented invention that may in any way be related thereto.

63-2-3

AS AD NO.

REPORT 1116-13

QUARTERLY STATUS REPORT

1 June to 31 August 1961

ANTENNA LABORATORY
DEPARTMENT OF ELECTRICAL ENGINEERING
THE OHIO STATE UNIVERSITY RESEARCH FOUNDATION
COLUMBUS 12, OHIO

Contract AF 19(604)-7270

Research
Initiated and Sponsored by

ASTROSURVEILLANCE SCIENCES LABORATORY
ELECTRONICS RESEARCH DIRECTORATE
AIR FORCE CAMBRIDGE RESEARCH LABORATORIES
OFFICE OF AEROSPACE RESEARCH
UNITED STATES AIR FORCE
BEDFORD, MASSACHUSETTS

1 September 1961

REPORT 1116-13

QUARTERLY STATUS REPORT

1 June to 31 August 1961

ANTENNA LABORATORY
DEPARTMENT OF ELECTRICAL ENGINEERING
THE OHIO STATE UNIVERSITY RESEARCH FOUNDATION
COLUMBUS 12, OHIO

Contract AF 19(604)-7270

Research
Initiated and Sponsored by

ASTROSURVEILLANCE SCIENCES LABORATORY
ELECTRONICS RESEARCH DIRECTORATE
AIR FORCE CAMBRIDGE RESEARCH LABORATORIES
OFFICE OF AEROSPACE RESEARCH
UNITED STATES AIR FORCE
BEDFORD, MASSACHUSETTS

1 September 1961

TABLE OF CONTENTS

QUARTERLY STATUS REPORT

A. PURPOSE

The change in the radar echo area of a satellite due to the plasma sheath, and the density and duration of satellite-induced ionization are being investigated.

B. ECHO AREA STUDIES

1. Introduction

A rapidly moving vehicle traveling through the ionosphere will disturb the distribution of charged particles and cause the electromagnetic properties of the vehicle to be modified. The scattering properties of such bodies in the perturbed ionized medium have been under investigation during the period June 1960 through June 1961.

The approach has been to determine the pertinent scattering mechanisms and to apply this knowledge in determining approximate methods for calculating the echo area. These methods have been applied to the simplified case of calculating the echo area of the concentric dielectric-clad sphere. This configuration was chosen since an exact solution for this echo area could be obtained and programmed on the IBM 704 computer. This exact solution was then used to find the region of validity of the approximate solutions that were evolved. It should be noted that the approximate solutions, once their limitations are understood, could then be applied to dielectric-clad bodies of arbitrary shape. No such extension is possible for the exact solution. The approximate solutions have been remarkably successful with only a few regions for which additional research is still required in order to find the desired echo area. These cases are outlined in this report.

An additional study has been instituted to find means of approximating the echo area of the dielectric body. This is essential since knowledge of this echo area is assumed in the work discussed above. In the solutions discussed, the exact echo area of the dielectric sphere has been used. However, for arbitrary shapes no such solution exists. While there has been a great deal of effort directed toward finding the echo area of metallic structures, there has been little effort devoted toward the case of dielectric bodies. The present effort in the latter field closely parallels that of finding the approximate solutions for the dielectric-clad bodies and appears to be equally successful. Once this effort is concluded, it should be possible to compute the echo area of multilayered bodies of rather arbitrary configuration with reasonable assurance. In fact, similar

techniques should be applicable to any electromagnetic phenomena involving a dielectric medium.

All of the techniques for finding the echo area to date have involved theoretical methods. It appears desirable to evolve experimental methods for determining these echo areas. Since the dielectric medium is a plasma, the relative dielectric constant can be less than unity. Thus an attempt is being made to design a radar scattering range for which the ambient medium is a liquid dielectric material with a dielectric constant significantly greater than that of free space. Then the lower dielectric constant of the plasma medium can be modeled. There are significant problems involved in the design of such a scattering range which are discussed in this report.

2. Computer Programs for Exact Echo Area of Dielectric and Dielectric-Clad Bodies

In order to determine the effect of a plasma sheath upon the scattering properties of several geometrically simple bodies and to aid in the development and evaluation of approximate methods which could be applied to more complex scatterers, the exact solutions for scattering by various spherical and cylindrical configurations have been programmed for the IBM 704 computer. A summary of these programs is given below.

(a) Conducting Sphere Surrounded by a Concentric Lossless Dielectric Shell

Multipole-expansion coefficients for the scattered field in the region outside the sphere are computed by Cramer's rule and are summed with the appropriate angular functions to give the far field E-field and the echo area. The program is single precision with no check for loss of validity resulting from roundoff error or from loss of significant digits due to subtraction of two nearly equal numbers which sometimes occurs. In general, valid results are obtained for the region of present interest, i.e., for radii up to about 2 wavelengths, and for dielectric constants up to about 4.0, but the program should be used with caution beyond this range.

In addition to the input parameters, which are the sphere and shell radii, r_1/λ_2 and r_2/λ_2, and the relative permittivity and permeability, ϵ_1/ϵ_2 and μ_1/μ_2, the program print-out includes:

Expansion coefficients for the scattered field outside the sphere, the far-field E-field, real and imaginary parts,

$|E|^2$,
echo area ($\sigma/\pi r_2^2$),
$\log_{10}$ (echo area), and
bistatic angle, θ,
for bistatic angles from 0° to 180° in 10° increments and for both E-plane and H-plane scattering.

Card output giving the input parameters, bistatic angle, and $\log_{10}$ (echo area) is available for use with card sorting and processing equipment and an automatic point plotter.

The echo area of plain conducting spheres may be computed with the program by setting $r_2/\lambda_2 = r_1/\lambda_2$ and/or $\epsilon_1/\epsilon_2 = \mu_1/\mu_2 = 1.0$.

(b) Homogeneous Dielectric Sphere

This program is identical to (a) above, except for the necessary reformulation of the calculation of multipole expansion coefficients.

(c) Two Concentric Right-Circular Cylinders of Arbitrary Composition (Normal Incidence)

Expansion coefficients for the scattered fields in all regions are calculated by matrix inversion. The resulting matrix is then re-inverted and compared with the original matrix as a check on the error incurred. The program is written in double precision, and its range of validity appears to be somewhat greater than that of the sphere programs, (a) and (b) above.

In addition to the input parameters, which are the cylinder and shell radii, r_1/λ_3 and r_2/λ_3, and the relative permittivities and permeabilities, ϵ_1/ϵ_3, ϵ_2/ϵ_3, μ_1/μ_3, and μ_2/μ_3, the print-out includes:

expansion coefficients for the scattered field in all regions,
the far-field E-field (parallel polarization)
and the far-field H-field (perpendicular polarization)
$|E|^2$ (parallel polarization)
and $|H|^2$ (perpendicular polarization),
echo width ($\sigma/4r_2$),
$\log_{10}$ (echo width), and
bistatic angle ϕ

for bistatic angles from 0° to 180° in 5° increments, for both parallel and perpendicular polarization of the incident wave with respect to the axis of the cylinder. Card output giving the input parameters, bistatic angles, and $\log_{10}$ (echo width) is available.

Echo areas of plain conducting cylinders, homogeneous dielectric cylinders, and conducting cylinders having a concentric dielectric shell are special cases which may be computed with this program.

(d) Echo Area Versus Frequency for a Conducting Sphere Having an Ion or Electron Shell, Immersed in the Ionosphere

Dielectric constants of the shell and of the ambient media and the inner and outer radii in terms of wavelengths in the ambient media, are computed as a function of frequency for given values of electron density and sphere radii. From these values, the scattered E-field and echo area are computed as in (a) above.

Print-out and card output are the same as for program (a) except that the sphere and shell radii, r_1 and r_2, and the electron densities of the shell and the ambient media, N_1 and N_2, are included. The range of validity corresponds to that of program (a).

3. Approximate Echo Area of Dielectric-Coated Spheres

The techniques developed previously to obtain the echo area of dielectric-clad bodies are being extended to explain certain discrepancies between the exact and the approximate solutions. Once all of the discrepancies are eliminated, these methods should be applicable to any dielectric-clad configuration. It would then seem advisable to program the computer to handle the approximate methods.

To review briefly the approximate methods used to determine the echo area of the dielectric-clad body, consider Fig. 1. The approximate echo area is obtained by a superposition principle for which the components are the reflected E-fields from the dielectric sphere alone and from the modified inner sphere. The inner sphere is modified by considering the refraction at the dielectric-free space interface. These two components are then combined vectorially. In general, these approximations have yielded results which are in remarkable agreement with the exact echo area.

One case for which a discrepancy had been noted earlier consists of a metal sphere $0.15\ \lambda_2$ in radius with a dielectric coating for which $\epsilon_r = 0.75$. The original approximate solution for this case is significantly in error, as may be noted in Fig. 2. These errors are eliminated by considering the change in path length introduced by the dielectric medium. This correction yields a modified approximate echo area which is in good agreement with the exact echo area, as shown by Fig. 2.

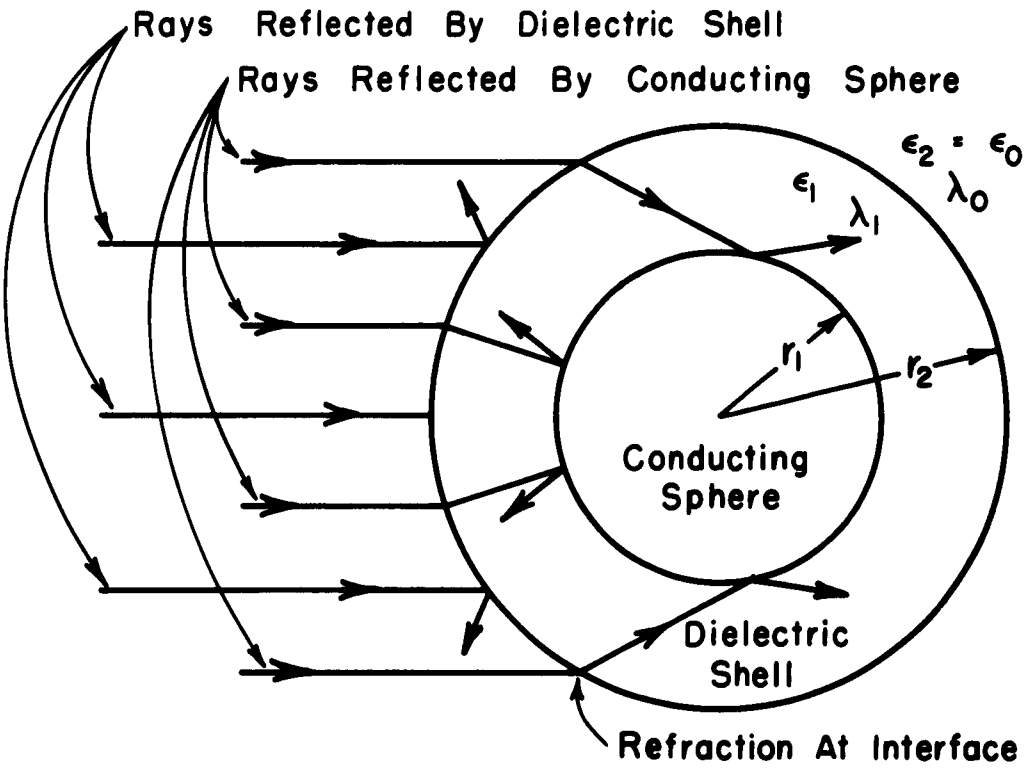

Fig. 1. Illustration of the reflection mechanisms for a dielectric-coated sphere.

This additional approximation eliminates all significant discrepancies which have been found for metal spheres of radius $r_1 \leq 0.15\,\lambda_2$ except for those having dielectric shells with relative dielectric constants on the order of $\epsilon_r = 4.0$. The chief difficulty in this case probably lies in the focusing properties of the dielectric sphere as illustrated in Fig. 3, and its solution most likely will be found by the study of these properties as discussed in a later section of this report.

While the inner spheres considered to date have been in and below the resonance region for which the most difficulties were anticipated, several cases of larger spheres are being considered. The exact echo areas of two of these cases are shown in Figs. 4 and 5. The approximate solutions also shown are not as yet satisfactory. In general the echo area of the dielectric sphere is sufficiently low so that it is not likely to be the reason for the deviation. Thus the source of error appears to lie in the refracted energy reflected from the inner sphere back toward the radar system or in multiple-bounce effects between the sphere and the dielectric shell. This problem is being examined further.

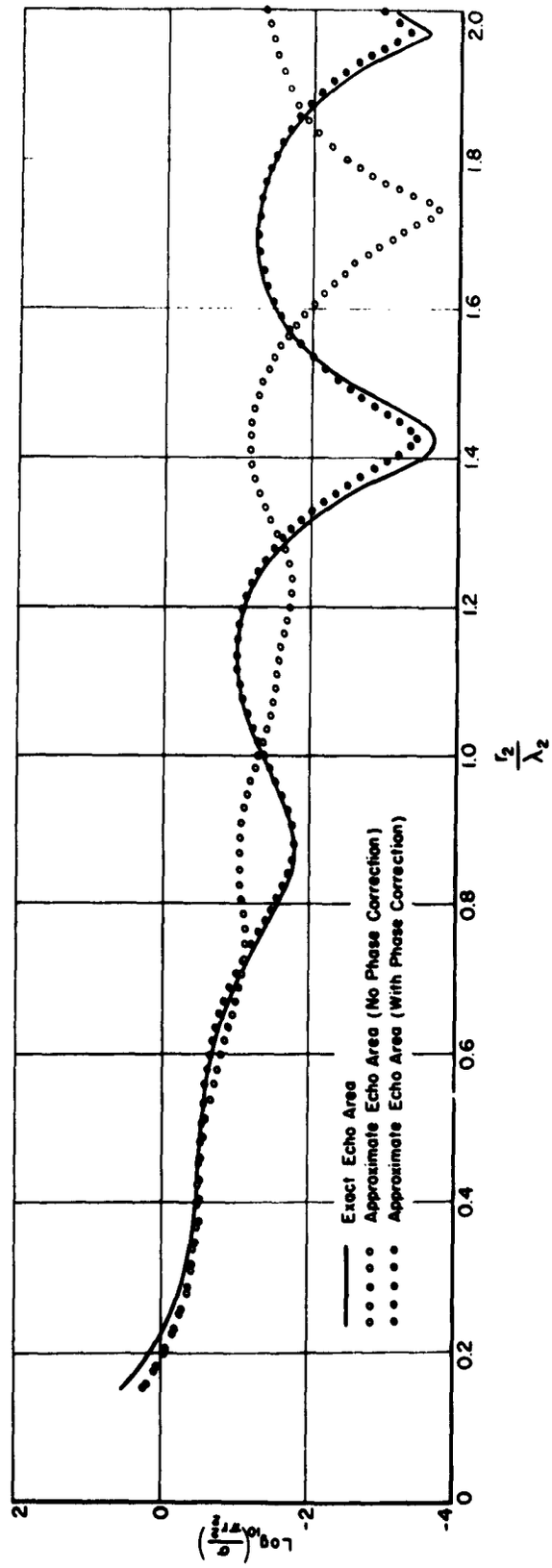

Fig. 2. Exact and approximate echo areas as a function of shell radius for a conducting sphere of radius $r_1/\lambda_2 = 0.15$ having a dielectric shell of $\epsilon_r = 0.75$.

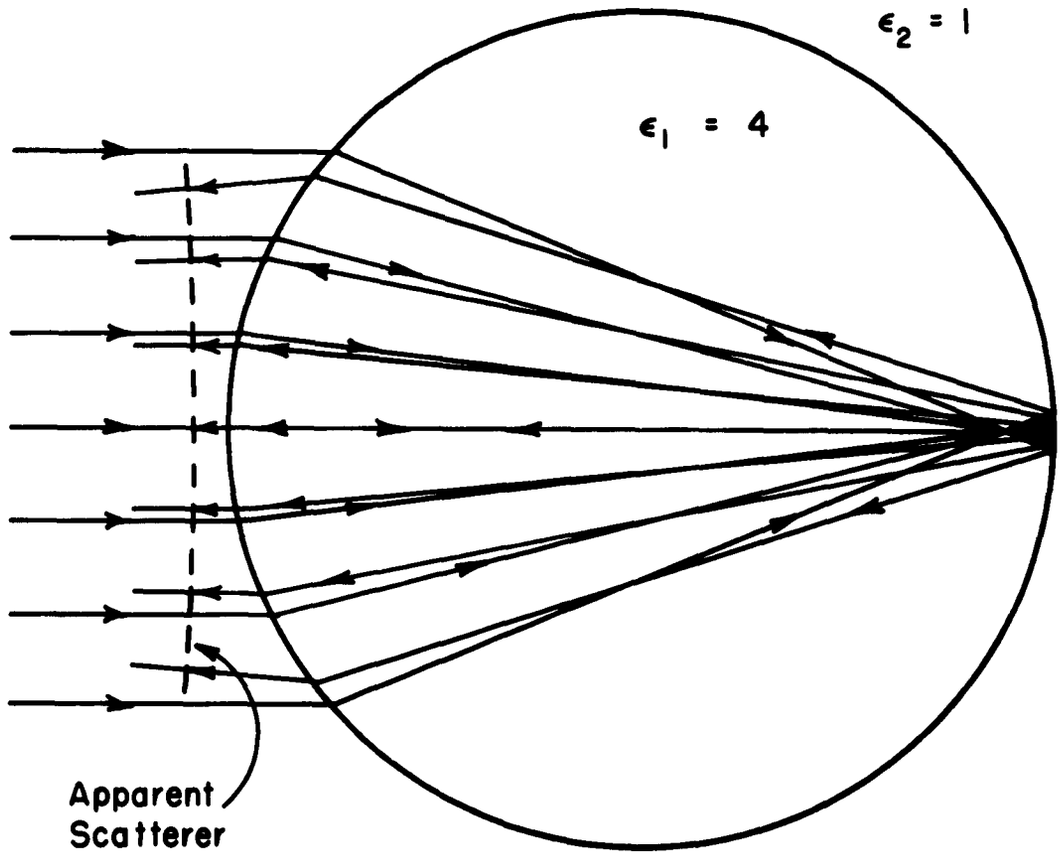

Fig. 3. Apparent reflecting surface for a critical dielectric constant of $\epsilon_r = 4.0$ as obtained by means of ray optics.

These problems appear at present to be the remaining ones that are of significance to complete treating dielectric-clad bodies by use of such approximate methods. It remains to obtain good techniques for calculating the echo area of dielectric bodies and then applying these methods to configurations other than a single concentric layer. Research has been initiated in both of these areas and is described in a later section of this report.

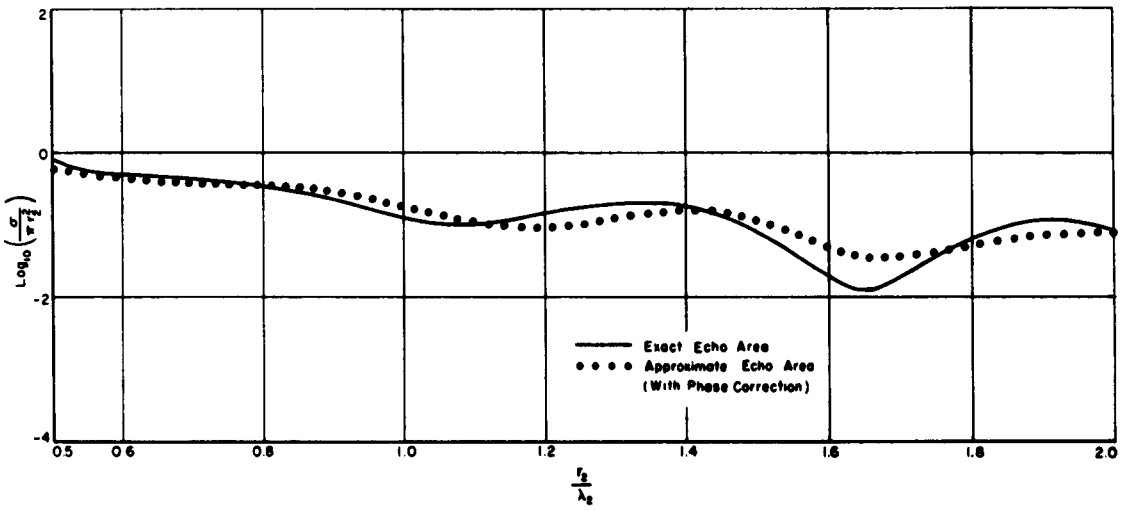

Fig. 4. Exact and approximate echo areas as a function of shell radius for a conducting sphere of radius $r_1/\lambda_2 = 0.50$ having a dielectric shell of $\epsilon_r = 0.75$.

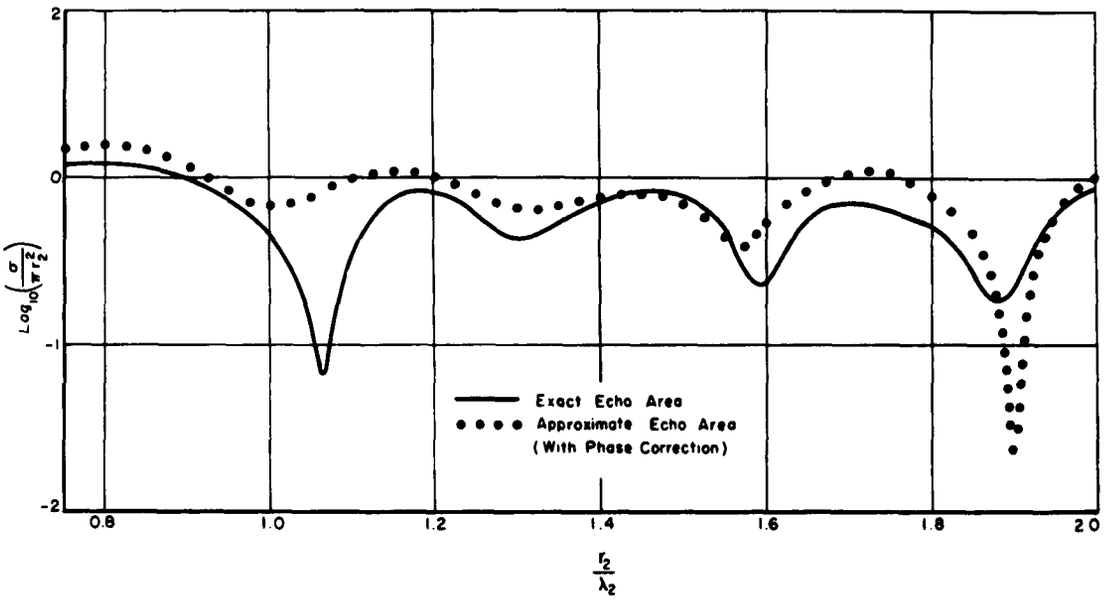

Fig. 5. Exact and approximate echo areas as a function of shell radius for a conducting sphere of radius $r_1/\lambda_2 = 0.75$ having a dielectric shell of $\epsilon_r = 1.50$.

4. Approximate Echo Area of Dielectric Bodies

It has, in general, been necessary to use the exact solution for the echo area of the dielectric sphere when obtaining the approximate solution for the dielectric-clad sphere. This represents a serious limitation if these methods are to be extended to calculate the echo area of dielectric-clad bodies of arbitrary shape. Thus techniques are being considered for obtaining the echo area of homogeneous dielectric bodies.

As in the case of the dielectric-coated body, the approach being used consists of determining the pertinent physical mechanisms and applying them to find the required echo area. The dielectric sphere is taken as the body to which the techniques are to be applied, since the exact echo area of these bodies has already been programmed on the computer available at Ohio State.

Various approximate methods are being considered. All involve two components, which are:

(1) Approximation of the front-face reflection by the product of the geometrical optics solution and the power reflection coefficient R to obtain

$$\sigma_F = (\pi a^2) \; R$$

where

$$R = \left(\frac{1 - \sqrt{\epsilon_r}}{1 + \sqrt{\epsilon_r}} \right)^2$$

and $\epsilon_r = \epsilon_1 / \epsilon_o$ is the relative dielectric constant of the sphere.

(2) Approximation of the reflection σ_R from the rear face using one of several methods, each usable for a specific range of values.

A phase delay is then introduced with the back-face reflection to obtain the total echo area

$$\sigma_D = \left| \sigma_F^{\frac{1}{2}} + \sigma_R^{\frac{1}{2}} \; e^{j\theta_s} \right|^2$$

where $\theta_s = (2\pi/\lambda)\, 4\sqrt{\epsilon_r}\, a$ is the phase delay of twice the sphere diameter (the approximate electrical path length).

To find the component of echo area σ_R due to the rear interface, a study of the apparent shape of the rear face was instituted. Note from Fig. 6 that a point P on the back side of the sphere appears to be at the point P'. It is desired to find the locus of P' and the radius of curvature r_c of this locus at P = (1, 0). This is done by applying Snell's law at the dielectric - free space interface and determining the apparent distance

$$L' = \sqrt{\epsilon_r}\, L ,$$

thus fixing the apparent rear surface. The apparent radius of curvature r_c at the point P = (1, 0) can then be obtained as

$$r_c = \frac{\sqrt{\epsilon_r}}{\sqrt{\epsilon_r} - 2} .$$

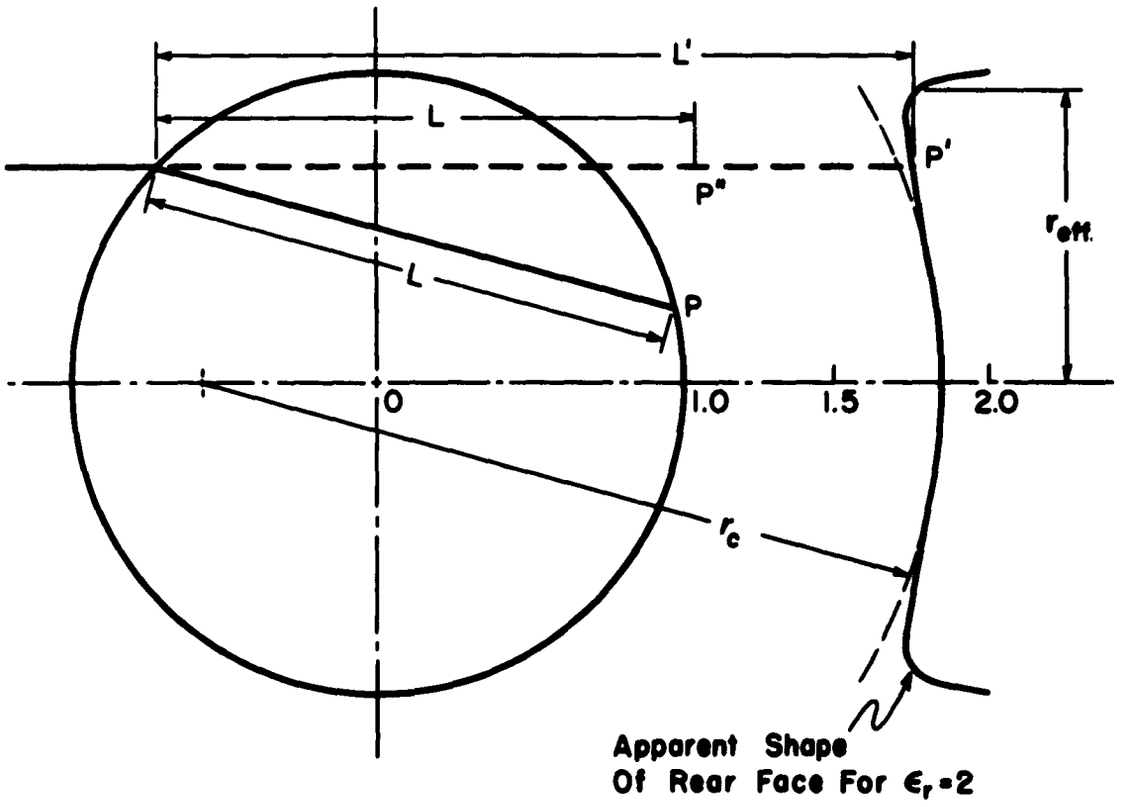

Fig. 6. Apparent position of the rear surface of a dielectric sphere.

A plot of $|r_c|$ vs. ϵ_r is given in Fig. 7.

For $\epsilon_r < 1$ the radius of curvature is less than 1, so that a valid approximation is found merely by considering the rear face to be a sphere of radius $r = a|r_c|$. Thus, for $\epsilon_r < 1$,

$$\sigma_R = \pi (a r_c)^2 T^2 R$$

where $T = 1 - R$ is the power transmission coefficient. The total reflection is

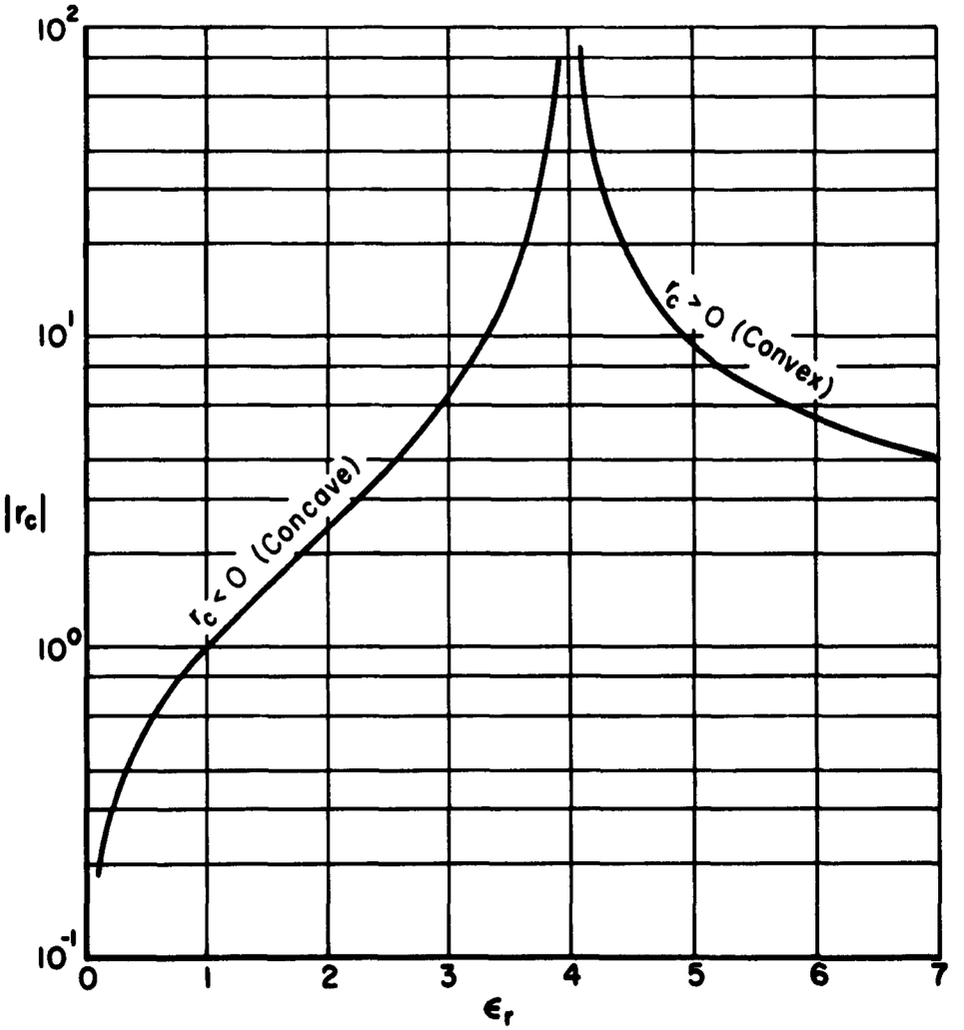

Fig. 7. Apparent radius of curvature, r_c, at the point $P = (1, 0)$ vs. relative dielectric constant ϵ_r.

$$\sigma_D = \pi a^2 R \left| 1 + T_{rc} \, e^{j\theta_s} \right|^2 .$$

An example of the validity of this approximation is furnished for $\epsilon_r = 0.25$ in Fig. 8. The discrepancies for $a/\lambda < 0.5$ are due to the fact that the large-sphere geometrical optics approximation has been used; hence agreement is not expected in this region. Nota that the plot of the echo area of a metal sphere in the region of Rayleigh scattering adjusted by the reflection coefficient behaves very well up to the first resonant peak. A combination, as yet unexplained, is then needed to connect the two approximations.

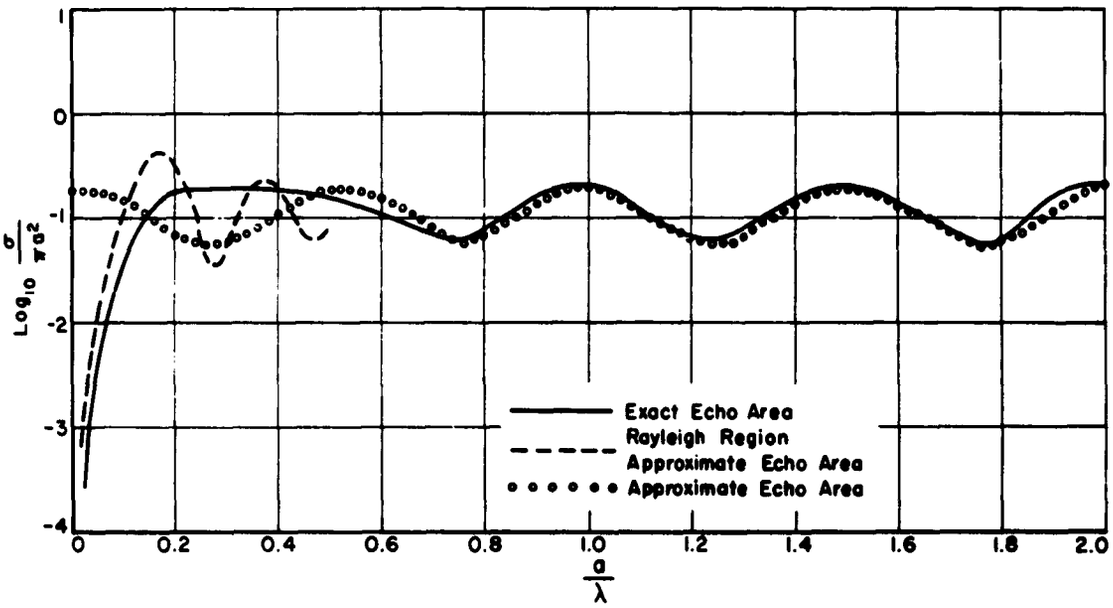

Fig. 8. Comparison of approximate echo areas with the exact echo area of a dielectric sphere for which $\epsilon_r = 0.25$.

For $\epsilon_r > 1$, the approximation becomes considerably more involved. The apparent radius of curvature is now large, which means that for small values of a/λ the rear face looks substantially like a flat plate. A plot of this apparent surface for $\epsilon_r = 2$ is given in Fig. 6. For $a/\lambda < 1$ the rear face appears to be a flat plate of radius $r_{eff}/a \approx 0.975$, for which the echo area is

$$\sigma_R = \frac{4\pi R T^2}{\lambda^2} \left(\pi a^2 \frac{r_{eff}^2}{a^2} \right)^2 .$$

This approximation is shown in Fig. 9, showing excellent agreement for $a/\lambda < 1$. (Again notice the Rayleigh region approximation.) For $a/\lambda > 1$, the apparent rear face might be approximated by two parts: (1) an annular ring, and (2) a concave reflector. Work is continuing on this and other explanations for scattering from dielectric bodies. The methods described work remarkably well, and it is hoped that extensions of them will make it possible to estimate the echo area of any dielectric body with reasonable accuracy.

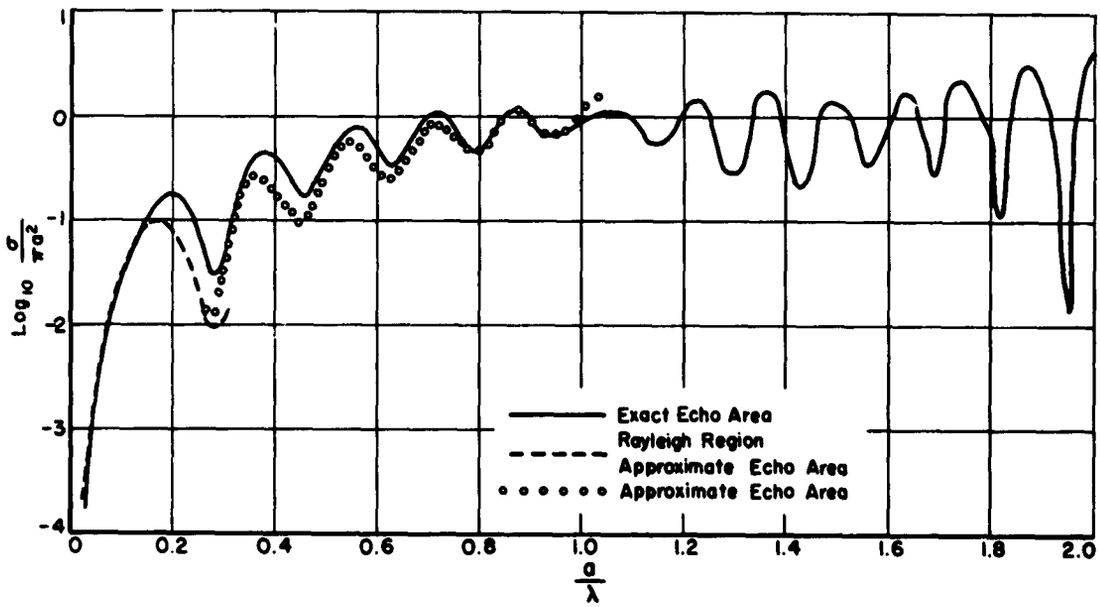

Fig. 9. Comparison of approximate echo areas with the exact echo area of a dielectric sphere for which $\epsilon_r = 2.0$.

5. Echo Area of Nonconcentric Spheres

The possibility of applying the approximate methods developed to more general problems is one of the major advantages of this approach. One simple problem that can not be solved by means of any exact solution is the metal sphere enclosed in a non concentric spherical shell

as shown in Fig. 10. The echo area for this configuration can be approximated as before by the square of the vector sum of the E-fields reflected from the dielectric sphere and from the modified metallic sphere. The relative phase of the two components would be obtained from the path length in the dielectric coating, the only problem for this case being to calculate the apparent diameter of the inner sphere. This is done from geometrical considerations in the following manner.

The inner sphere shown in Fig. 10 is a metallic conductor. The outer sphere is dielectric material with relative dielectric constant ϵ_1. Assume ray 1 and ray 3 to be tangent to the inner sphere. Then from geometry,

$$R_o \sin \theta_1 + a \sin \left[\beta - (\theta_o - \theta_1) \right] = R_1$$

Similarly, for ray 3,

$$R_o \sin \theta_1' = a \sin \left[\beta + (\theta_o' - \theta_1') \right] = R_1 .$$

These relations plus Snell's law yield expressions for sin θ_o and sin θ_o', for given values of a, R_1, R_o, β.

The apparent diameter D of the inner sphere is then given by

$$D = \overline{PR} + \overline{P'R'} = R_o (\sin \theta_o + \sin \theta_o') .$$

The solution for the echo area for this type of configuration is to be verified experimentally for a dielectric constant $\epsilon_1 > 1$. As yet no technique has been evolved for measuring the echo area of bodies when $\epsilon_1 < 1$, as occurs for many plasma-coated configurations. One possible method for such measurements is discussed in the following section.

6. The Oil-Tank Experiment

Research has been initiated to determine the optimum parameters of a scattering range to measure the echo area of a plasma-coated body. The suggested approach is to construct a tank filled with a liquid dielectric material to act as the ambient medium. The plasma coating could then be modeled by using a dielectric material whose relative dielectric constant is less than that of the liquid, thus simulating a dielectric coating of dielectric constant less than 1.

To date, no liquid has been found to satisfy the requirements for such a range; however, there are numerous possible materials yet to be

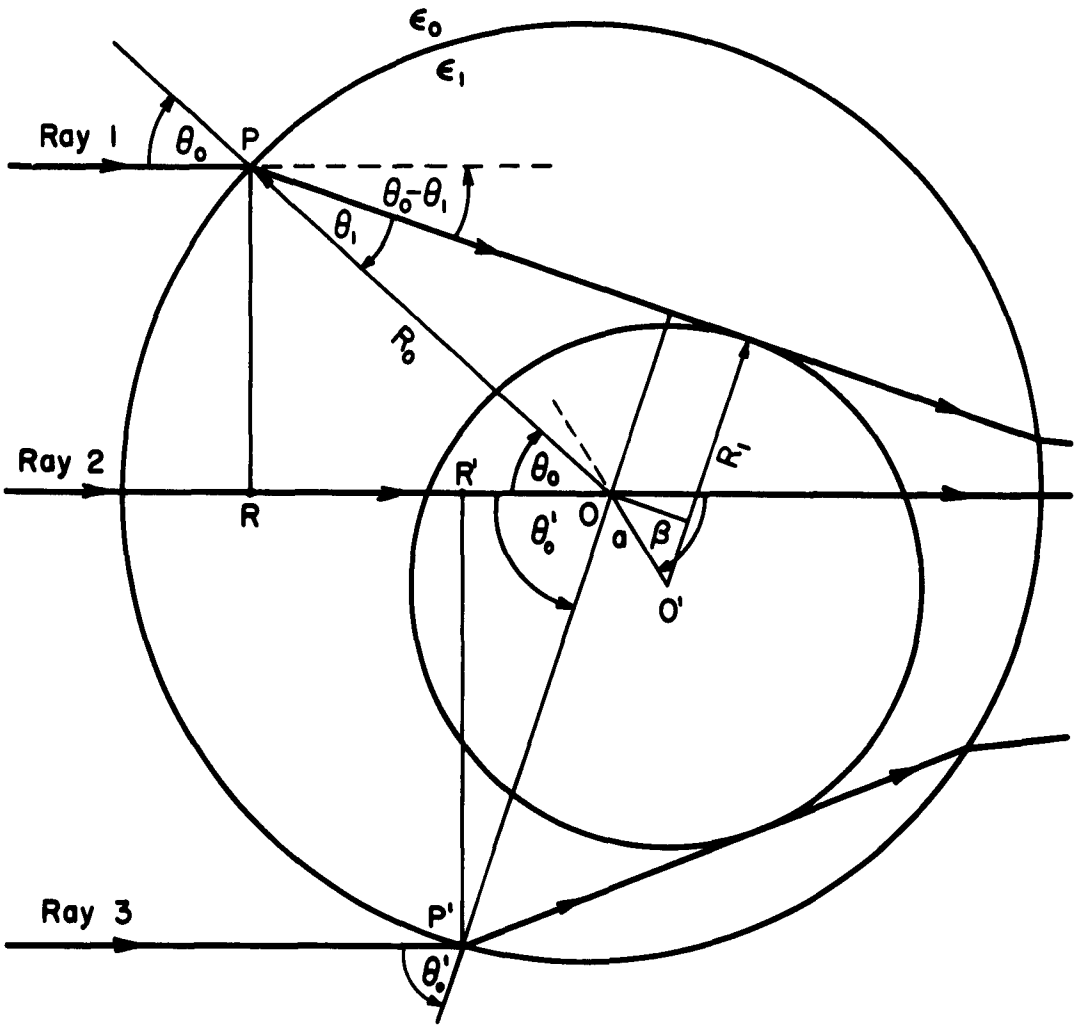

R_0 – Radius Of Outer Sphere
R_1 – Radius Of Inner Sphere
O – Center Of Outer Sphere
O' – Center Of Inner Sphere
a – Distance $\overline{OO'}$ Between Centers Of Inner And Outer Spheres
β – Angle Between Line OO' And Direction Of Propagation

Fig. 10. Construction for the calculation of the apparent diameter of nonconcentric spheres.

examined. The requirements are: (1) a relative dielectric constant on the order of 4 or greater, and (2) a loss tangent less than 0.01 , at a frequency of about 3000 Mcs. Considering the size of satellites in orbit and the plasma frequency of the ionosphere, model sizes must range from 0.05 λ to 0.5 λ. A frequency much higher than 3000 Mcs would present model size problems while a lower frequency would make the range size prohibitive.

A completely enclosed system containing in the liquid the antenna(s) and scattering body is essential to minimize nulling problems which already are severe because of the small model size. A study of patterns in the Fresnel region of a rectangular aperture indicates the minimum usable range from antenna to model to be about 10 λ. Assuming the relative dielectric constant of the liquid to be 4.0, this minimum dimension at 3000 Mcs is 0.5 meter. A cylindrical tank of 0.5-meter radius would require about 250 gallons of liquid. Cost of the liquid must, therefore, be considered.

The most fundamental problem encountered is that of dielectric losses. The attenuation factor is given by

$$\alpha = 27.3\ D \text{ db/wavelength}$$

where D is the loss tangent of the dielectric liquid. Since the path length for the reflected signal will be about 20 λ , the transmission loss will be approximately

$$L = 546\ D \text{ db.}$$

Because of the small echoes expected from the scattering bodies, maximum permissible transmission loss is estimated to be 5 db. Therefore, the loss tangent of the liquid must be less than 0.01.

Present efforts are directed toward finding a liquid which meets the above requirements. Reported data in the frequency range of interest is inadequate, and so properties of possible suitable liquids are being measured. If necessary, an attempt will be made to synthesize a material having the desired properties by doping a low-loss liquid with a powder of high dielectric constant material. It is hoped that this will increase the dielectric constant without prohibitively increasing loss tangent.

C. DENSITY AND DURATION OF SATELLITE-INDUCED IONIZATION

1. Electron Distribution in the Ionosphere

A prerequisite to the knowledge of the intensity and duration of satellite-induced anomalies in the ionosphere is a knowledge of the ambient electron density in the ionosphere. The electron density below the F_2-layer maximum is generally known from the virtual height ($h'(f)$) curves obtained from sweep-frequency ionosoundings. In addition, a method [1] has been proposed for obtaining this same information from average virtual-height curves (average of ordinary and extraordinary).

The electron density above the F_2-layer maximum, however, is still relatively unknown. Therefore, continued effort has been made toward obtaining electron densities by the Faraday polarization-rotation method in conjunction with Earth satellite 1959 Iota I at altitudes of 573 km to 1115 km. Data which were taken during the period September 1960 to February 1961 are being analyzed. A report [2] is being prepared presenting the values obtained for the integrated electron densities to the satellite for passes of the satellite quite near Columbus. In addition, correlation of these values of the integrated electron densities with magnetic disturbances, as well as with values of the integrated electron densities below the F_2 maximum, are presented.

Further insight into the separation of the Faraday polarization rotation due to the integrated electron density, N_h, from that due to the electron density in the vicinity of the satellite, N_s, has been made possible through the use of a digital computer program. In fact, it is found that the peak in the Faraday rotation period need not appear at near approach, as was reported previously.[3] To illustrate this point, the relationship between the time rate of change of the Faraday polarization rotation and the electron density is presented. It is:

$$(1) \qquad \frac{f^2}{K}\frac{d\theta}{dt} = \frac{\partial \bar{M}}{\partial t}\int_0^{h_s} N\,dh + \bar{M}\int_0^{h_s}\frac{\partial N}{\partial t}\,dh + N_s\,\bar{M}\cos\xi\,\frac{dr}{dt}$$

where

$d\theta/dt$ = the time rate of change of the Faraday polarization rotation
K = 2.97×10^{-2} in MKS units
f = the satellite transmitting frequency
$\bar{M}$ = $H \cos\phi \sec\xi$ at a mean height
H = magnetic field strength
ϕ = angle between the magnetic field and the direction of propagation

ξ = angle between the zenith and the direction of propagation at the satellite

h_s = satellite height

N = number density of electrons

dr/dt = the time rate of change of range

N_s = number density of electrons at the satellite.

In the analysis $\partial N/\partial t$ is assumed to be negligible since the ionosphere is assumed to be spherically stratified.

The relationship between $d\theta/dt$ and the measured nulls due to the polarization rotation relative to a fixed linear antenna is

$$\left|\frac{d\theta}{dt}\right| = \left|\frac{\pi}{T}\right|$$

where T is the time between the nulls and is called the Faraday half-period. On solving Eq. (1) for T with the $\partial N/\partial t$ term neglected, one finds

$$(2) \qquad |T| = \frac{\pi/\partial\bar{M}/\partial t}{N_s}\left|\frac{1}{\frac{N_h}{N_s} + \frac{\bar{M}}{\partial\bar{M}/\partial t}\cos\xi\,\frac{dr}{dt}}\right| .$$

Thus, it is seen from Eq. (2) that if $\frac{\bar{M}}{\partial\bar{M}/\partial t}$ is a constant which can have either a positive or negative sign, then the half-period has the shape described by

$$(3) \qquad |T| = \frac{\pi\Big/\frac{\partial\bar{M}}{\partial t}}{N_s}\left|\frac{1}{B + C\cos\xi\,\frac{dr}{dt}}\right|$$

where

$B = N_h/N_s$

$C = \dfrac{\bar{M}}{\partial\bar{M}/\partial t}$ and

$B/C = \dfrac{N_h}{N_s}\,\dfrac{\partial\bar{M}/\partial t}{\bar{M}}$.

Thus, fora particular pass where $\bar{M}$ and $\partial\bar{M}/\partial t$ are known, it is the

ratio of the integrated electron density to the local electron density which determines the shape of the T curve versus time of passage over the observing station. The possible shapes for a particular pass are shown in Fig. 11 for various ratios of B to C. It is seen from Fig. 11 that for a particular pass the position of the peak in the plot relative to the time of the closest point of approach is dependent upon the ratio of B to C or N_h to N_s. This fact allows order of magnitude values of N_s to be found once N_h has been determined. This analysis, however, neglects the effects of refraction, path splitting, electron density horizontal gradients, and ionospheric irregularities.

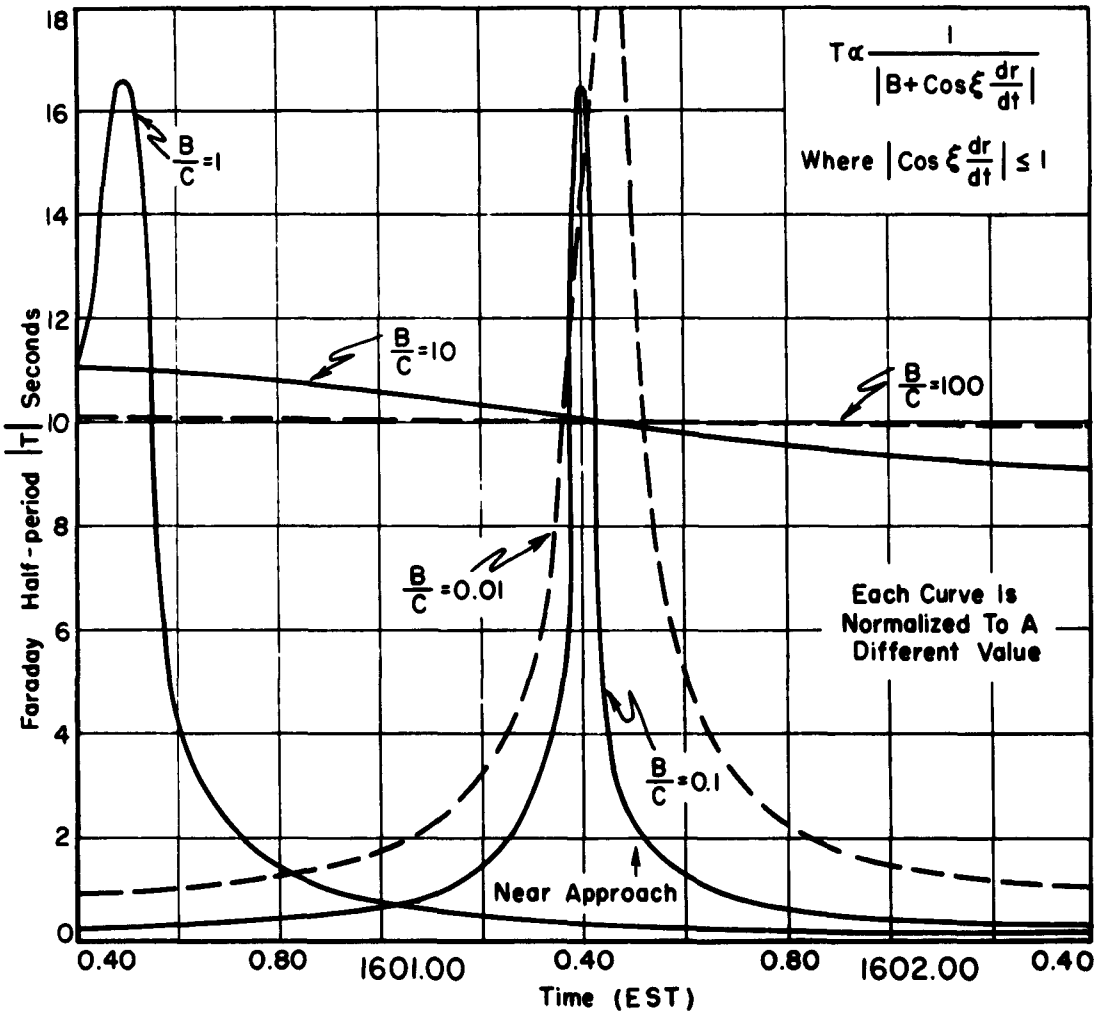

Fig. 11. Typical variations of the Faraday half-periods for a pass of Explorer VII.

Studies of the electron density above the maximum have been quite ambiguous to date because the satellites in orbit have not been designed to transmit on enough low frequencies to provide good raw data for analysis. A definite need exists for satellites with multiple phase-locked frequencies in the frequency range 10-50 Mc. In fact, using a sweep frequency from 8 Mc to say 100 Mc, in an idealized situation Unz [4] has shown that it is possible to obtain a polynomial expansion for the index of refraction or the electron density as a function of height above the F_2 maximum.

2. Cessation of Scintillation Studies

High correlation [5] of the amplitude scintillation of 1959 Iota I with the ionospheric spread F has indicated that this phenomenon is not associated with any satellite-ionosphere interaction. Therefore, further studies of this phenomenon have been discontinued.

D. PROGRAM FOR NEXT INTERVAL

Investigation of approximate techniques for calculating the echo areas of dielectric-coated spheres will be continued with emphasis upon eliminating the discrepancies which remain for shells of high dielectric constant and for spheres of large radius. Among the techniques to be employed are calculation of the equivalent shape of the front face of the conducting sphere resulting from the refracted ray paths through the dielectric shell, consideration of nonuniform illumination of the conducting sphere due to refraction of the incident wave by the dielectric shell, and consideration of multiple-bounce effects between the conducting sphere and the air-dielectric interface.

The approximate techniques will be applied to the calculation of bistatic echo areas of dielectric-coated spheres and to the calculation of monostatic and bistatic echo areas of dielectric-coated cylinders during the next interval. The results obtained will be compared with exact values obtained by means of the computer programs which are now completed. The approximate methods will also be applied to the case of a sphere enclosed by a nonconcentric shell of $\epsilon_r > 1$, and the results will be checked against appropriate model measurements. The practicability of writing a computer program for calculating approximate echo areas will be investigated.

Additional methods for calculating the echo areas of homogeneous dielectric bodies will be studied. Consideration will be given to the

possible extension of physical optics and variational techniques, and of other methods which have been used successfully for conducting bodies, to the case of homogeneous dielectric bodies.

Dielectric constant and loss tangent measurements directed toward finding a suitable liquid for use in the proposed oil-tank scattering range will be continued. If this investigation has a successful outcome, design and construction of the scattering range will be initiated during the next interval.

Analysis of the 6 months of Explorer VII data will be continued, with special emphasis upon describing long-term (lasting more than one day) ionospheric irregularities.

More raw data from satellite radio signals will be taken if any new satellites with desirable frequencies are launched. Theoretical studies will be continued into possible means of obtaining further physical information (e.g., electron densities at the satellite, horizontal gradients of electron density, and vertical gradients of scale height) from either the present data or any new raw data such as would be available from the NASA S-45 Earth satellite.

BIBLIOGRAPHY

1. Unz, H., "Simplified Analysis of Ionospheric h'(f) Records Using Wave Refractive Index", Report 1116-12, August 1961, Antenna Laboratory, The Ohio State University Research Foundation; prepared under Contract AF 19(604) 7270 with Astrosurveillance Sciences Laboratory, Air Force Cambridge Research Laboratories.

2. Potts, B.C. (unpublished work).

3. Quarterly Status Report, Report 1108-2, 16 November 1960, Antenna Laboratory, The Ohio State University Research Foundation; prepared under Contract AF 19(604) 7270 with Astrosurveillance Sciences Laboratory, Air Force Cambridge Research Laboratories.

4. Unz, H., "On the Evaluation of Electron Density Distribution in the Outer Ionosphere by Satellite Radio Signals", Report 1116-11, August 1961, Antenna Laboratory, The Ohio State University Research Foundation; prepared under Contract AF 19(604) 7270 with Astrosurveillance Sciences Laboratory, Air Force Cambridge Research Laboratories.

5. Final Engineering Report 1108-6, Antenna Laboratory, The Ohio State University Research Foundation; prepared under Contract AF 19(604)7270 with Astrosurveillance Sciences Laboratory, Air Force Cambridge Research Laboratories.